

NUMERICAL INVESTIGATION OF HEAT TRANSFER THROUGH POROUS MEDIA

Rafel Hekmat Hameed

Babylon University / College of Eng. / Mechanical Eng. Dept.

ABSTRACT

Heat transfer mechanism model was predicted in order to simulate the temperature distribution of the two phases (glass-air) through the macrostructure of porous media sample in depth 20 mm at local equilibrium. It has been heating the sample from left side through x-axis with different values of heat flux. The model contain two stages: firstly, predict the temperature distribution in solid phase by transient 2-dimensional conduction heat equation; secondly, switching was happened in the program to simulate the temperature distribution in fluid phase of sample by energy balance.

It has been found the temperature distribution in glass and air through the first two layers of series configuration of the sample. It showed very small values of heat transfer coefficient between these layers. That means high insulation property was observed from this structure of porous media sample.

Due to the heating process, it has been noted the air inside the first layer was accelerated a very little bit as marks the onset of convection. This is due to the pressure gradient was produced between the outside and inside layers of sample through heating process with time. Darcy law was used to calculate this air velocity. Heat transfer coefficient inside porous media, effective Nusslet number and Nusslet number of fluid phase were calculated.

Key words: Porous Media; Heat Transfer Mechanism; Heat Transfer Coefficient; Air Velocity; Mathematical Model; Temperature Distribution.

الخلاصة :-

تم عمل نموذج رياضي لتوضيح توزيع درجات الحرارة خلال البنية الداخلية لنموذج مادة مسامية مكونة من الزجاج والهواء وبسمك 20 ملم بافتراض حالة الاتزان بين الطورين (زجاج-هواء). تم تسخين نموذج المادة المسامية من الجهة اليسرى للمحور السيني لاتجاه النموذج المسامي بقيم مختلفة من الفيض الحراري. تمت النمذجة على مرحلتين المرحلة الأولى هو حساب حساب درجة الحرارة في الطور الصلب (الزجاج) بواسطة استخدام معادلة التوصيل الحراري ثنائية البعد بتغير الزمن والمرحلة الثانية حساب التوزيع الحراري لطور المائع (الهواء) باستخدام معادلة الطاقة بافتراض اتزان الطاقة بين الطورين.

تم إيجاد التوزيع الحراري لدرجات الطور الصلب (الزجاج) وطور المائع (الهواء) خلال الطبقتين الأولىيتين للبنية الداخلية لتكوين المادة المسامية، وقد اتضح إن معامل انتقال الحرارة قليل جدا بين طبقة الزجاج وطبقة الهواء وهذا يعني ان المادة المسامية لديها قابلية على العزل الحراري.

بسبب عملية التسخين لوحظ ان الهواء الموجود داخل طبقات البنية التركيبية للنموذج المسامي وخاصة في الطبقة الأولى يتحرك بسرعة بطيئة جدا نتيجة حدوث عملية انتقال حرارة بالحمل اللحظي وهذا يرجع بسبب حدوث فرق بقيم الضغط بين سطح الطبقة الخارجية المسخنة للنموذج المسامي والطبقة الداخلية التي تحتوي على الهواء خلال عملية التسخين بتغير الزمن، استخدم قانون دارسي لحساب قيمة سرعة الهواء اعتمادا على قيم تغير الضغط. تم حساب معامل انتقال الحرارة ورقم نسلت المؤثر للمادة المتسامية ولطور المائع (الهواء) في المادة المتسامية أيضا.

Nomenclature

c_p	Specific heat at constant pressure. [J/kg.°C]
i, j	Indices increase along x, and y axes.
k_e	Effective thermal conductivity of porous media. [W/m °C]
k_f	Thermal conductivity of fluid phase. [W/m °C]
k_s	Thermal conductivity of solid phase. [W/m °C]
K	Permeability. [m ²]
Nu_e	Effective Nusselt number of porous media.
Nu_f	Nusselt number of fluid phase (air).
Re	Reynold number.
t	Time. [second]
T	Temperature. [°C]
u	Velocity. [m/s]
q''	Heat flux. [W/m ²]
α_e	Effective thermal diffusivity. [m ² /s]
$(\rho c_p)_e$	Effective heat capacity of porous media. [J/m ³ .°C]
$(\rho c_p)_f$	Effective heat capacity of fluid. [J/m ³ .°C]
$(\rho c_p)_s$	Effective heat capacity of solid. [J/m ³ .°C]
λ	Convergence factor.
\emptyset	Porosity.
μ	Dynamic viscosity . [kg/m.s]

1. INTRODUCTION

An understanding of heat transfer and fluid flow in porous media is important in many engineering fields, such as soil mechanics, powder metallurgy, chemical processing, petroleum reservoir recovery, and high performance insulation for building and power collection.

In a fluid-saturated porous medium, the thermal diffusivity of the fluid phase may be much lower or higher than that of the solid structure. In transient heat conduction processes within such porous media, the assumption of local thermal equilibrium must be discarded, as pointed out by (Kaviany, 1995). Also, there are a number of steady situations in which the heat transfer process cannot be regarded as being in local thermal equilibrium. When there is a significant heat generation occurring in any one of two phases (either solid or fluid), the temperature in the two phases are no longer equal. The assumption of local thermal equilibrium cannot be used when he analyze the entrance region of packed column where a hot gas flows at high speed.

(Kladias and Prasad, 1991) conjectured that agreement could be improved by considering separate energy transport equations for the individual phases. This hypothesis, however, would then imply that local thermal equilibrium is no longer valid. But this appears to contradict their previous conclusion that conduction through the solid phase has a stability effect on the fluid. In other words, conduction heat transfer through both phases is promoted. Beginning with a two-equation model for transient heat conduction in a two-phase porous media. They used volume averaging and judicious assumptions to reduce the general governing equations for conduction heat transfer in a two-phase porous medium to a single governing equation for the spatially averaged temperature. The numerical solutions to the closure equations were then used to compute the effective thermal conductivity tensor for each spatially periodic unit cell. The representative cell types were for continuous and discontinuous

fluid phases. The continuous fluid phase model approximated a porous medium in which the solid particles either do not make contact, or point contact. The discontinuous fluid phase model, on the other hand, incorporated the effects of particle-to-particle contact through empirical parameters.

(Hus, 1999) proposed a simplified two-energy equation model for transient heat conduction in porous media, and assessed the validity of the assumption of local thermal equilibrium. The major difference between his form and the classical form is the appearance of additional coupling terms accounting for thermal tortuosity, which are related to the temperature gradient in the other phase. He treated not only conduction but also convection in porous media. Having established the macroscopic energy equations for both phases, useful exact solution are obtained for fundamental heat transfer processes associated with porous media, namely, steady conduction in a porous slab with internal heat generation within a solid, and also, thermally developing flow through a semi-infinite porous medium.

(Whitaker, 1999) described that the basic difficulty encountered in the analysis of energy transport and fluid flow in porous media is that both phenomena depend heavily upon the microstructure of the porous media. If one were to assume that this sample is sufficiently large, so that the continuum assumption is valid for both the solid and fluid phases. Then, it is perfectly reasonable to formulate the differential forms of the conservation equations for energy within the two phases. The result is a pair of coupled partial differential equations. Difficulties arise when characterizing the interfacial boundary condition for the two phase system. In the case of conduction heat transfer, for example, matching heat fluxes and temperatures at the solid-fluid interface is an essential boundary condition. Unfortunately, this boundary condition is a function of the geometry of the solid-fluid interface; hence difficulties arise in modeling the interface geometry. As a result, the analysis of transport processes in porous media on the microscopic level is inherently intractable.

In the present work, a mathematical model was simulated the conduction-convection heat transfer in order to calculate the temperature distribution through the macroscopic structure layers in porous media sample. Input data of effective thermal properties, permeability, and porosity of porous media sample were assumed in this model. Air velocity was calculated by using Darcy's law.

2. MATHEMATICAL MODEL

In a macroscopic analysis, the entire porous media is treated as a continuum of average microscopic variables. One means of formally defining average macroscopic variables from microscopic variables occupying a representative elementary volume, such as the one pictured in Fig. 1-a, is the method of volume averaging.

The use of macroscopic variables leads to the definition of effective properties which empirically account for the effects of the microstructure. It has been dependent upon the study by (Hans, 1999) which determined the minimum effective thermal conductivity occurs when the solid and fluid layers assume a series arrangement as shown in Fig. 1-b. The effective thermal conductivity is then given by:

$$\frac{1}{k_e} = \frac{\phi}{k_f} + \frac{(1-\phi)}{k_s} \quad (1)$$

And the effective thermal diffusivity was given as:

$$\alpha_e = \frac{k_e}{\phi (\rho c_p)_f + (1-\phi)(\rho c_p)_s} \quad (2)$$

ϕ is the porosity of glass-air media, this value was about 0.365, as reported by (Nield and Bejan, 1999).

When the fluid phase is in motion thermal energy transfer is coupled to the motion. It is the coupling of the phenomena of fluid flow and heat transfer which has led to many of the difficulties encountered in characterizing solid-fluid system when the fluid phase is in motion.

Numbers of an assumptions and simplification have to be made in order to solve the mathematical model:

1. A rectangular porous media sample was assumed with dimension (94 mm × 100 mm) as illustrated in Fig. 2.
2. The sample was a homogenous and isotropic.
3. It has been assumed a symmetrical about x-axis.
4. The initial condition $T(x, y, 0) = 25^\circ\text{C}$, and the boundary conditions assumptions as:

$$\text{At } x = 0 \quad , \quad -k_e \frac{\partial T}{\partial x} = \bar{q}$$

$$\text{At } y = b \quad , \quad \frac{\partial T}{\partial y} = 0 \quad ; \quad \text{symmetrical about x-axis.}$$

5. The left surface through y-axis was heated by two values of heat flux \bar{q} 80 W/m², and 150 W/m².
6. Temperature at the right side was maintained at ambient temperature 25°C.
7. The top and lower surfaces through x-axis were adiabatic.
8. All points laying on the boundary a, b, d, and f call boundary nodes, while the rest of point of grid c, and e are called internal nodes.
9. It has been assumed the thickness of solid layer as 14 mm, and air layer thickness as 4 mm, and 6 mm respectively in macroscopic structure of porous media sample.

The number of nodes in solid phase (glass) (M×N) are (14×50), while in fluid phase (air) are (6×50), and (4×50) respectively.

Firstly, the model using the two-dimensional time-dependent heat equation to predict temperature distribution through the layers of solid phase as shown in Fig. 2. The heat transfer equation was used as:

$$\frac{\partial^2 T}{\partial x^2} + \frac{\partial^2 T}{\partial y^2} = \frac{1}{\alpha_e} \frac{\partial T}{\partial t} \quad (3)$$

- 1) At point a where $x = y = 0$; upon the boundary conditions were assumed as shown in Fig. 3 , where $i=1$ to 1, $j=1$ to 1. Then eq. (3) becomes

$$T_{ij}^{n+1} = 4\lambda T_{ij+1} + (1 - 6\lambda)T_{ij} + 2\lambda T_{i+1j} + 4\lambda \bar{q} \frac{\Delta y}{k_e} \quad (4)$$

Where $\lambda = \frac{\alpha_e \Delta t}{\Delta y^2}$, as the convergence factor.

- 2) The temperature distribution through y-axis was employed upon the boundary conditions were assumed as shown in Fig. 4, where $i=1$ to 1, $j=2$ to N-1. The new form of eq. (3) becomes

$$T_{ij}^{n+1} = \lambda T_{ij+1} + (1 - 4\lambda)T_{ij} + \lambda T_{ij-1} + 2\lambda T_{i+1j} + 2\lambda \bar{q} \frac{\Delta y}{k_e} \quad (5)$$

- 3) Through x-axis as shown in Fig. 5, where $i=2$ to 14, and $j=1$ to 1, then eq. (3) becomes

$$T_{ij}^{n+1} = \lambda T_{i+1j} + (1 - 4\lambda)T_{ij} + \lambda T_{i-1j} + 2\lambda T_{ij+1} \quad (6)$$

- 4) At corner b where $i=1$ to 1, and $j=N$ to N as shown in Fig. 6, then eq. (3) represents as:

$$T_{ij}^{n+1} = 2\lambda T_{ij-1} + (1 - 4\lambda)T_{ij} + 2\lambda T_{i+1j} + 2\lambda \bar{q} \frac{\Delta y}{k_e} \quad (7)$$

- 5) At inside plane of solid phase as shown in Fig. 7, where $i=2$ to 14, and $j=2$ to N-1 eq. (3) becomes:

$$T_{ij}^{n+1} = \lambda T_{i+1j} + (1 - 4\lambda)T_{ij} + \lambda T_{i-1j} + \lambda T_{ij+1} + \lambda T_{ij-1} \quad (8)$$

- 6) Through the line insulated as shown in Fig. 8, Where $i=2$ to 14, and $j=N$ to N, then eq. (3) represents as:

$$T_{ij}^{n+1} = 2\lambda T_{ij-1} + (1 - 4\lambda)T_{ij} + \lambda T_{i+1j} + \lambda T_{i-1j} \quad (9)$$

Secondly, the mathematical model switching to energy eq.(10) in order to calculate the temperature distribution in fluid phase (air). This was done due to the assumption of two phases are in local thermal equilibrium in macroscopic structure of porous media. (Hans, 1999) shows the energy equation is employed to account for the effects of fluid motion, this energy equation as:

$$(\rho c_p)_e \frac{\partial T}{\partial t} + (\rho c_p)_f u \frac{\partial T}{\partial y} = k_e \left(\frac{\partial^2 T}{\partial x^2} + \frac{\partial^2 T}{\partial y^2} \right) \quad (10)$$

Where u is the air flow velocity inside the porous media macroscopic structure as shown in Fig. 2, this was calculated by Daracy's law, which was detailed below in section 2.1.

The energy eq. (10) can be written in finite difference time dependent form as:

$$(\rho c_p)_e \frac{T_{ij}^{n+1} - T_{ij}^n}{\Delta t} + (\rho c_p)_f u \frac{T_{i+1j}^n - T_{ij}^n}{\Delta x} = k_e \left(\frac{T_{i+1j}^n - 2T_{ij}^n + T_{i-1j}^n}{\Delta x^2} + \frac{T_{ij+1}^n - 2T_{ij}^n + T_{ij-1}^n}{\Delta y^2} \right) \quad (11)$$

Where $\lambda = \frac{\alpha_e \Delta t}{\Delta x^2}$ is convergence factor, then eq.(11) becomes

$$T_{ij}^{n+1} = \lambda T_{i-1j} + \left(1 - 4\lambda + \frac{(\rho c_p)_f}{(\rho c_p)_e} u \frac{\Delta t}{\Delta x} \right) T_{ij}^n + \lambda T_{i+1j} + \left(\lambda - \frac{(\rho c_p)_f}{(\rho c_p)_e} u \frac{\Delta t}{\Delta x} \right) T_{i+1j} + \lambda T_{ij-1} \quad (12)$$

Equation (12) was used to simulate the temperature distribution of void space in fluid phase (air) inside the macroscopic structure of sample at two dimensions as shown in Fig. 9.

The temperature distribution through x-axis of fluid phase inside the macroscopic structure was shown in Fig. 10. The new form of eq. (10) becomes

$$T_{ij}^{n+1} = \lambda T_{i-1j} + \left(1 - 4\lambda + \frac{(\rho c_p)_f}{(\rho c_p)_e} u \frac{\Delta t}{\Delta x} \right) T_{ij}^n + \left(\lambda - \frac{(\rho c_p)_f}{(\rho c_p)_e} u \frac{\Delta t}{\Delta x} \right) T_{i+1j} + 2\lambda T_{ij+1} \quad (13)$$

2.1. Calculation the Air Flow Velocity inside Porous Media Sample.

(Nabovati and Sousa; 2007) showed in this approach, air flow is simulated in the inter-grain region and inside the pores of the porous media by using Darcy law over the domain. By using a pressure gradient, through assuming the air flow in x-direction namely:

$$u = \frac{K}{\mu} \left(-\frac{dp}{dx} \right) \quad (14)$$

Where K is the permeability, and it was calculated by using the Carman and Kozeny equation as:

$$K = \frac{d_p^2 \phi^3}{150(1-\phi)^2} \quad (15)$$

Table (1) represents the calculation value of velocity and Reynolds number dependent upon the value of pressure gradient and the value of permeability at two values of a void space assumption 4 and 6 mm. The Δp calculates as physically the difference pressure between surface sample (i.e. point 1) and in the middle of a void space of air inside the sample (i.e. point 2) as shown in Fig. 11. At initial condition points 1 and 2 are at value of atmospheric pressure.

It has been shown through heating process by heat flux, the pressure already increased at the surface of the sample (i.e. point 1). While the pressure at void space (i.e. point 2) remains at atmospheric pressure. Then, it can be assume different values of pressure gradient through heating to predict velocity value of air flow inside void space. The distance dx represents between point 1 at surface sample, and point 2 at the middle of a void space assumption.

(Michele, 2010) showed that Darcy eq. (14) is only valid when Darcy velocity u is sufficiently small. Reynolds numbers up to 10 may still be Darcian for porous media flow is typically expressed as:

$$Re = \frac{\rho u d}{\mu} \quad (16)$$

Where ρ is the density of air, u is Darcy velocity of air, d is a representative grain diameter for the porous media, and μ is the viscosity of air. Then, Reynolds numbers which were calculated through the two values of air flow velocity inside porous media sample were presented in table (1). These values were small and still being Darcian.

It has been investigated through the simulation model, the onset heat transfer coefficient by Newton law for a two values of heat flux as:

$$h = \bar{q}/\Delta T \quad (17)$$

Where $\Delta T = T$ surface of solid phase – T bulk of fluid phase

Also the Nusselt number based upon the stagnant effective thermal conductivity Nu_e and the Nusselt number upon the fluid thermal conductivity Nu_f were calculated and presented in table (2).

3. RESULTS AND DISCUSSION

Figures 12 and 13 show the thermal history of heat transfer mechanism in porous media through the macrostructure of porous media sample (glass and air). It was shown the spatial temperature distribution through x-axis in first solid and fluid layer respectively of the macrostructure of the sample, which were assumed these layers in a series arrangement. In the macroscopic analysis, the solid layer thickness was 14 mm, while the fluid layer was 4mm and 6mm. The temperature distribution was simulated by using two values of heat flux 80 W/m^2 and 150 W/m^2 .

It has been shown the temperature was decreased far away from the surface, when the heat flux was fixed. It has been pointed a maximum value of temperature was predicted at the point surface (i.e. $x=0$), which was about $770 \text{ }^\circ\text{C}$, and $1425 \text{ }^\circ\text{C}$ at time 300 seconds depending upon the values of heat flux, and heating time. This is due to this point was contact directly with the source of heat flux.

The temperature variation through the fluid layer dependent upon the void space (i.e. porosity), permeability, and the velocity flow of air inside the void space. This was affected by the value of heating, which produced different values of pressure gradient between the outside surface sample and inside the void space of sample. It has been shown the high value of spatial temperature, which was calculate in fluid phase at the first layer of air after the interfacial line. That means, it is the air layer that contact the upper surface of solid layer. Then, the temperature was decreasing with distance far away inside fluid layer. These results depending upon the time of heating, and the value of heat flux supply. It has been pointed a very little difference in temperature at fluid phase, when used a different values of void space. These results were presented at time 300 seconds.

Figures 14 and 15 illustrate the spatial temperature distribution of fluid layer at time interval 50 seconds by using energy equation. It has been shown high exponential response value predicted at time 300 seconds. It was pointed for every time interval that the temperature was higher at adhesive tape of the solid layer, and then decreasing as far away from this layer. These results were proportionality with the values of heat flux, air velocity inside the void space, and the time of heating. It was prescribed obviously that the difference in temperature values were a very little by assuming different values of void space, which was produced different values of air velocity.

Figures 16 and 17 illustrate an isothermal contour map of fluid layer at time 300 seconds with two values of heat flux, and two values of void space. It has been shown the thermal layer of air was developed above the upper surface of solid layer. These were growing with two values of heat flux, and the time of heating. These factors were accelerated the air with very slow flow velocity. These thermal layers were distorted and mark the onset of convection. The increasing value and time of heating were growing inside the air layer. Also, the higher value of heat flux and heating time were increasing the pressure gradient value, which was produced increasing in air flow velocity. That also effected with the void space dimension inside the microstructure of porous media sample. Fig. 17 indicated more growing of thermal layer than others. The air velocity starts to accelerate in the localized unstable points.

Figure 18 shows the surface contour of three dimension in fluid phase with heat flux 150 W/m^2 and time 300 seconds, air void space 6 mm, and air velocity 0.029. It has been shown more growing of thermal layer at the first tape of air layer that contact the upper surface of solid layer. It has a high distorted in thermal boundary layer was happened at the center point then other neighboring points.

These results were confirmed with theoretical work which was predicted by (Tan and Sam, 1999).

It has been seen, the values of Reynolds numbers depending upon the permeability and Darcy velocity of air values. Table (2) shows the calculation values of heat transfer

coefficients, effective Nusselt numbers of porous media (Nu_e), which was dependent upon effective thermal conductivity of two phases (glass-air), and the Nusselt numbers of fluid phase (air). It has been shown the value of onset of heat transfer coefficient which was decreasing with the value of a void space of fluid layer increasing with two values of heat flux. These results were consistent with the results detailed by (Michele, 2010).

CONCLUSION

1. The temperature distribution through solid phase (glass) and fluid phase (air) of porous media sample has been simulated at local equilibrium of two phases by building a computer program.
2. It has been found that the temperature values in solid phase (glass) higher than the temperature values in fluid phase (air). That means the heat transfer mechanism between glass and air was low in this microstructure of porous media sample. These results confirmed this structure of sample has a good insulation property.
3. The value of air velocity was simulated by Darcy law is in the range of 0.013 m/s to 0.029 m/s. These values depending upon the value of heat flux, which was produced the pressure gradient between the outside surface of sample and inside the void space of fluid.
4. The formation and development of the thermal layer at adhesive tape above the upper surface of solid layer show and mark the onset of convection, that was affected by heating value, heating time, and the air velocity inside the void space.

Table (1) values of velocity and Reynolds number calculated from Darcy law

Void space (mm)	Pressure gradient Δp (N/m ²)	Permeability K (m ²)	Velocity u (m/s)	Re
4	0.31325	1.2863×10^{-8}	0.0138	3.5226
6	0.31325	2.89387×10^{-8}	0.029	11.1039

Table (2) values of heat transfer coefficient, effective Nusselt number, and Nusselt number for fluid phase at 300 s.

Q W/m ²	Void Space mm	Velocity m/s	h W/m ² °C	Nu_e	Nu_f
150	4	0.0139	5.636	1.1887	3.1435
	6	0.029	4.7274	0.9971	2.63679
80	4	0.0139	5.433	1.1459	3.0303
	6	0.029	4.7273	0.9970	2.63674

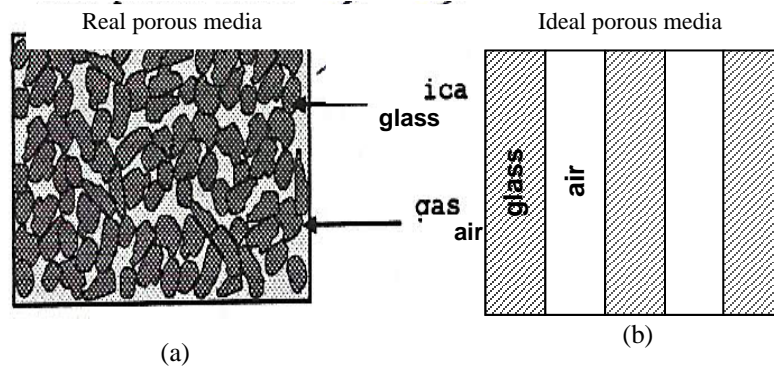


Fig. 1 Solid and fluid phases in series configuration (glass-air). (Hans, 1999).

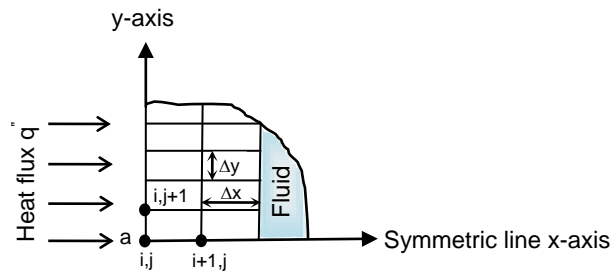


Fig. 3 Energy balance on boundary nodes of point a.

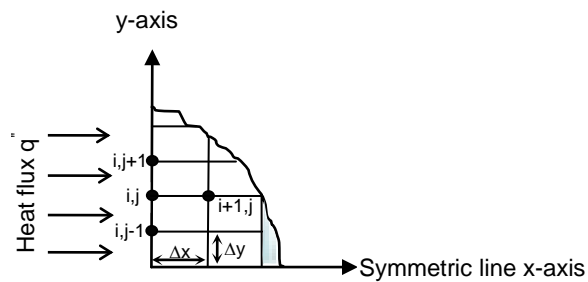


Fig. 4 Energy balance through y-axis.

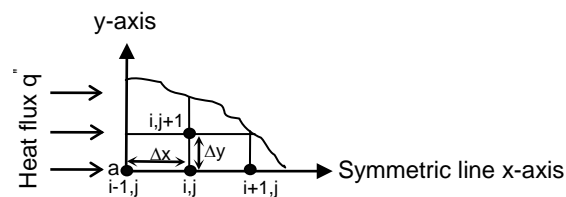


Fig. 5 Energy balance through x-axis.

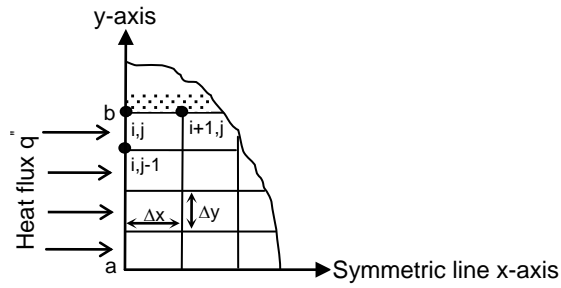


Fig. 6 Energy balance on boundary nodes of point b.

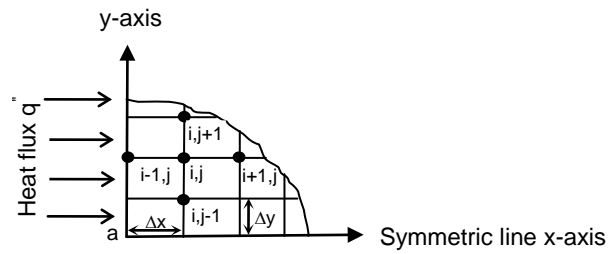


Fig. 7 Energy balance through inside nodes of solid phase.

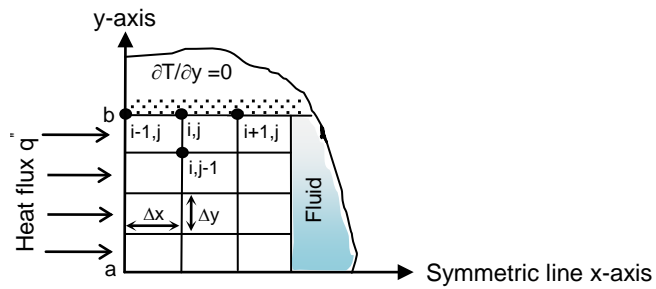


Fig. 8 Energy balance through insulated line.

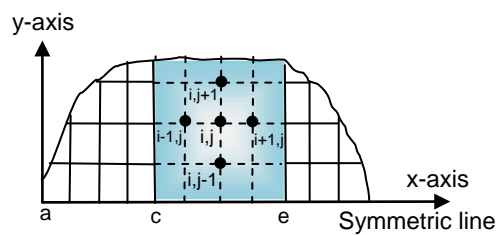


Fig. 9 Energy balance through internal points of fluid phase.

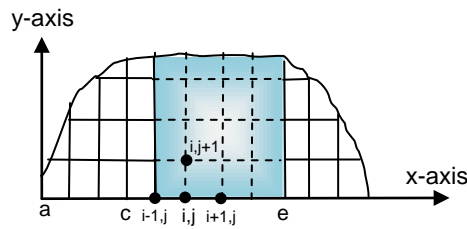


Fig. 10 Energy balance through x-axis of fluid phase.

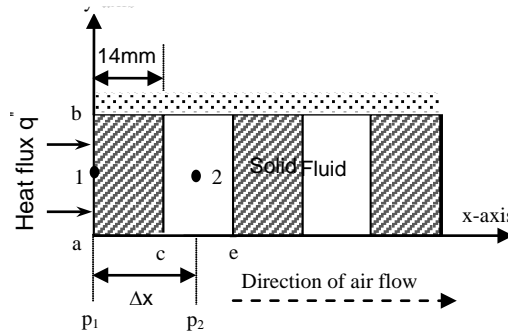


Fig. 11 Pressure gradient in porous media.

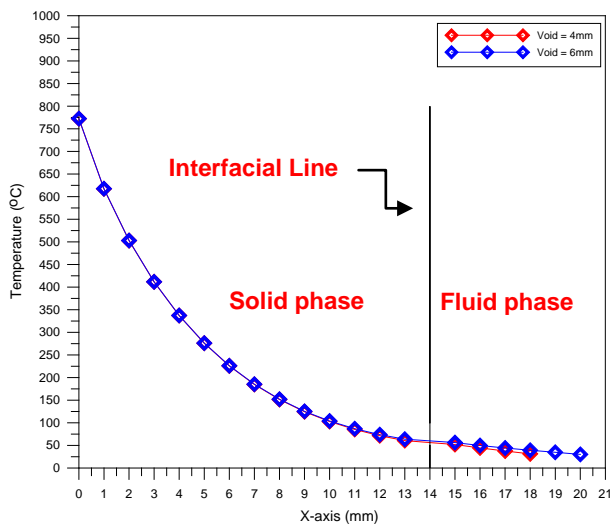


Fig. 12 Spatial temperature distributions in porous media sample through two phases with heat flux 80 W/m^2 , at time 300 seconds.

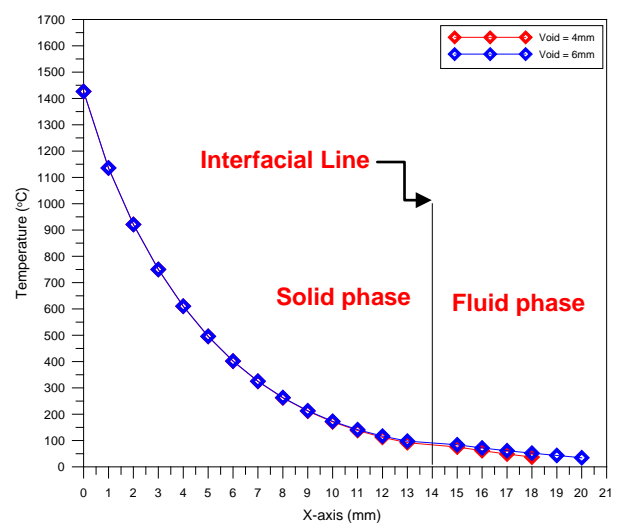


Fig. 13 Spatial temperature distributions in porous media sample through two phases with heat flux 150 W/m^2 , at time 300 seconds.

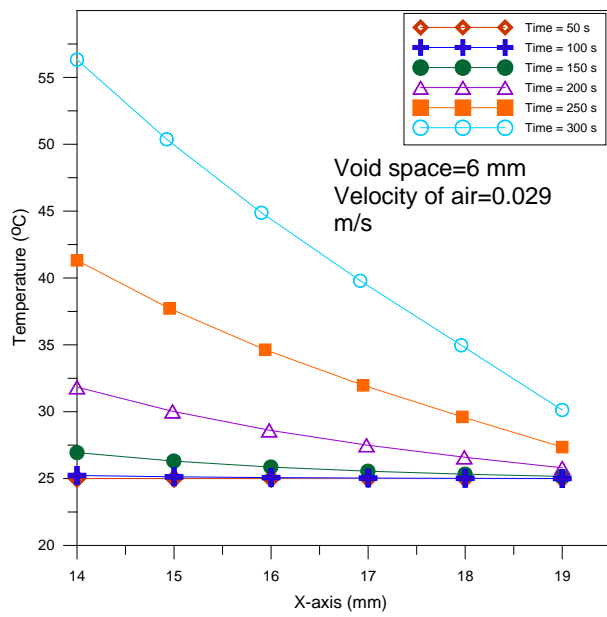


Fig. 14 Spatial temperature distribution of air layer at time interval 50 s, with heat flux 80 W/m^2 .

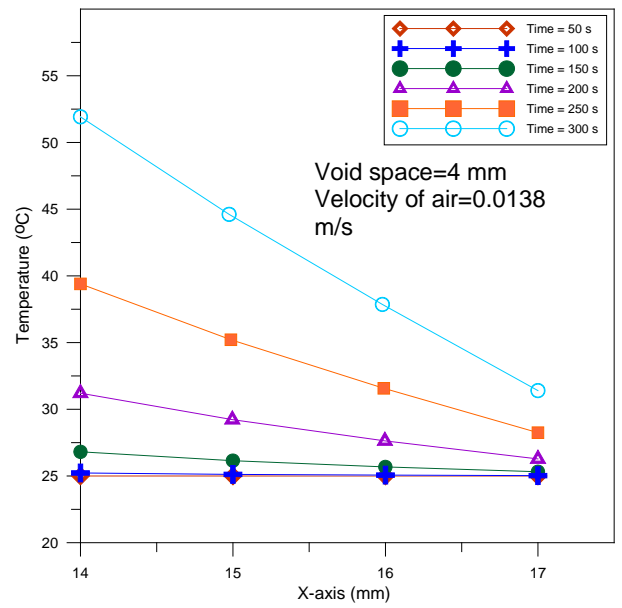


Fig. 15 Spatial temperature distribution of air layer at time interval 50 s, with heat flux 80 W/m^2 .

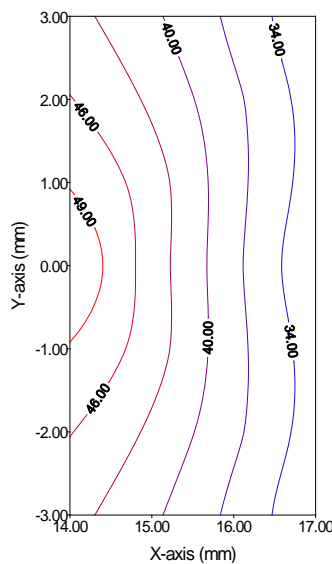
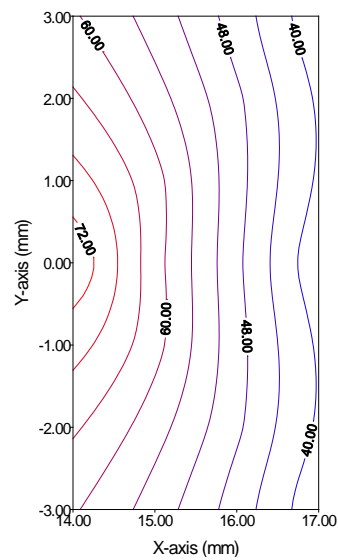
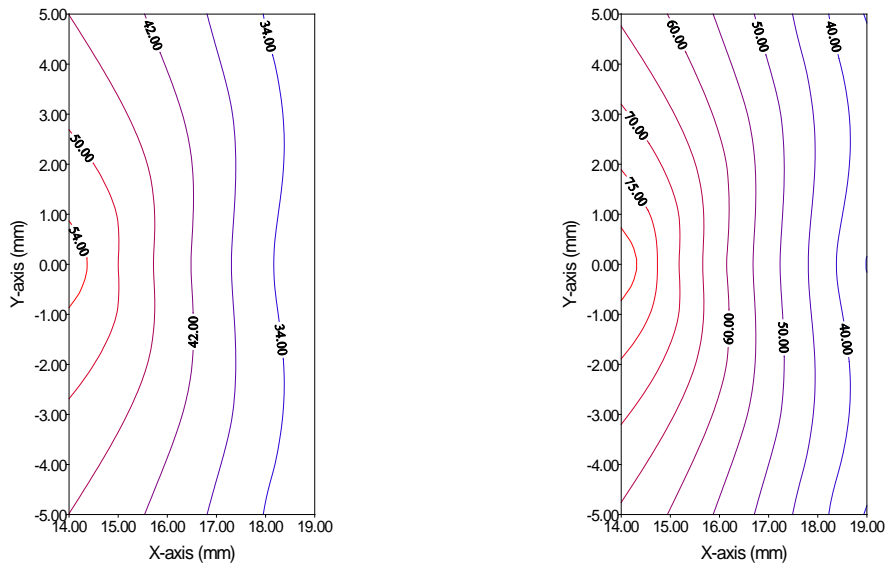


Fig. 16 Isothermal contour map of fluid layer at time 300 seconds, void space 4mm, and air velocity 0.0138 m/s.





$q''=80W/m^2$

$q''=150W/m^2$

Fig. 17 Isothermal contour map of fluid layer at time 300 seconds, void space 6mm, and air velocity 0.029 m/s.

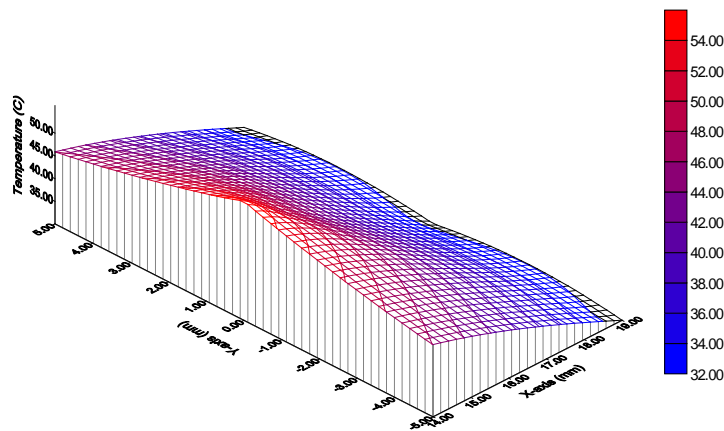


Fig.18 Surface contour of fluid layer in porous media at time 300 seconds with heat flux of 80W/m², void space 6mm, and air velocity 0.029m/s

5. REFERENCES

Hans, T., Aichlmayr, 1999, " The effect thermal conductivity of saturated porous media ", M.Sc. Thesis, University of Minnesota, Mechanical Eng. Department.

Hsu, C.T., 1999, " A closure model for transient heat conduction in porous media", J. Heat Transfer, Vol. 121, pp. 733-739.

Kaviany, M., 1995, " Principles of Heat Transfer in Porous Media", Book, 2nd ed., Springer, New York.

Kladias, N., and Prasad, V., 1991, "Experimental verification of Darcy-Brinkman-Forchheimer flow model for natural convection in porous media", Journal of Thermophysics and Heat Transfer, Vol.5, No.4, pp. 560-576.

Michele, celli, 2010, " Stability, viscous dissipation and local thermal non equilibrium in fluid saturated porous media", ph.D Thesis, University of Bologna, Italy.

Nabovati, A., Sousa, A.C.M., 2007, " Fluid flow simulation in random porous media at pore level using the Lattice Boltzmann method", Journal of Eng. Science and Technology, Vol.2, No.3, pp.226-237.

Nield, D.A., and Bejan, A., 1999, "Convection in Porous Media", Book 2nd edition, New York, Springer, Veriag.

Tan, ka kheng, and Sam. Torng, 1999, " Simulation of the onset of Transient Convection in Porous Media under Fixed Surface Temperature Boundary Conduction", 2nd International conference on CFD in the Minerals and process Industries, 6-8 December.

Whitaker, S., 1999, " The Method of volume Averaging", Book, Kluwer Academic publishers Dordrecht.